TCAD Simulation of CMOS Image Sensor

Z. M. Simon Li and Yegao George Xiao

Crosslight Software Inc Vancouver BC Canada

***Abstract* — TCAD simulation of CMOS active pixel image sensor from process to opto-electronic response is presented in this application note with a full suite of modeling software developed by Crosslight. The electronic responses are presented versus various power intensity, illumination wavelength, and aperture size effects, together with some OE/QE results. The presented results demonstrate a methodological and technical capability for 3D modeling optimization of complex CMOS image sensor.**

I. Introduction

With the popularity of smart phones and tablets with built-in cameras, CMOS image sensor (CIS) is experiencing growth by leaps and bounds. The market size for image sensors is expected to reach 17.5B USD and CIS is expected to account for a large market share of ~93% in 2020 [1].

As we will explain in this section, CIS is a complex optoelectronic device requiring full coupling of optical generation and carrier transport. Process and structural design is also important for achieving good performance. Therefore, TCAD simulation covering process simulation, optical field calculation, and electronic device simulation are necessary.

Historically, CMOS technology has been well understood and can be modeled with well-established commercial software for both process and device simulation, including tools from Crosslight Software [2,3]. Optical simulation by itself is also well established with finite difference time domain (FDTD) being the main methods [4]. However, researchers from the optical side rarely talk to those from the electrical or process side: such a lack of communication means that researchers from all sides miss opportunities to fully understand the physical effects that limit device performance. This application note is an attempt to bridge the gap between the electrical simulation and optical simulation by giving deeper insight into the working principle and TCAD design of CIS.

This note is organized as follows. We start with an overview of the software tools and basic theories which we will use when analyzing the CIS simulation. We shall use a simplified 2D structure with a pinned photodiode (PPD) and a transfer gate to explain the basic operation principle of a CIS unit. Next, more advanced analysis involving in effects of interface traps and AC analysis shall be described. Then, the 2D simulation will be completed by adding a reset MOSFET. The remaining part of this note will describe 3D simulation using advanced TCAD tools.

II. Basic Theories for CMOS Image Sensors

A comprehensive simulation of CIS requires a full suite of software tools for process, optical field computation and electrical device modeling. This application note will focus on interaction of optics and electronics after we give a brief overview of various software tools and related physical effects.

i) Process simulation

CIS relies heavily on MOSFET technology which traditionally has been simulated with process simulation software for processes such as diffusion and implantation. The simulation details of these processes have been described in the technical manual of Crosslight Csuprem [2] and in a book [5]. A full blown process simulator with CSuprem [2] generates the structure, mesh and doping distribution necessary for optical and device simulation later on.

ii) Optical simulation

Since the size of a CIS cell is comparable to wavelengths under detection, it is necessary to consider effect of diffraction. Finite difference time domain (FDTD) method is the preferred approach to compute the optical field under such conditions. The quantities being computed are optical efficiency and or quantum efficiency. The material dispersion parameters are used in the FDTD model to account for dispersion and loss.

Three dispersion models are supported by Crosslight FDTD models; the formulation of these models implies a certain convention for the time dependence of the optical fields. The Lorentz dispersion is in $\exp(-i\omega t)$ convention as with Eq. (1) for permittivity ϵ

$$\epsilon(\omega, \mathrm{x}) = \epsilon_\infty(\mathrm{x}) + \sum_n \frac{\omega_n^2 \Delta\epsilon_n}{\omega_n^2 - \omega^2 - i\omega\gamma_n}, \quad (1)$$

where ω is the frequency, X is the position, ϵ_∞ is the instantaneous permittivity, ω_n is the resonant frequency, $\Delta\epsilon_n$ is the magnitude of the resonance peak, and γ_n is the damping coefficient.

The Drude dispersion is in exp(+iωt) convention with permittivity as with Eq. (2).

$$\epsilon(\omega, \mathrm{x}) = \epsilon_\infty(\mathrm{x}) - \sum_n \frac{\omega_n^2}{\omega(\omega + i\gamma_n)}, \quad (2)$$

The Direct dispersion is in exp(+iωt) convention with permittivity as with Eq. (3).

$$\epsilon(\omega, \mathrm{x}) = \sum_n \frac{A_n}{B_n\omega^2 + C_n i\omega + D_n}, \quad (3)$$

where A_n, B_n, C_n and D_n are coefficients for each resonance peak.

Since FDTD requires that the grid spatial discretization must be sufficiently fine to resolve both the smallest electromagnetic wavelength and the smallest geometrical feature in the model, very large computational domains may be required, which results in very long solution times. Models with long, thin features, (like wires) are difficult to model in FDTD because of the excessively large computational domain required.

For front illuminated CIS, it is necessary to consider light blocking effects from interconnect metal wires and this makes FDTD rather inefficient. Therefore, much research has long been focused on parallelization of FDTD code. Crosslight CLFDTD [4] offers an option to run on graphic processing unit (GPU), which may increase the speed by up to one hundred times.

For the purpose of seeing physical trend in a short time, a simpler plane wave model can also be used. The method for plane wave model is the transfer matrix method (TMM) and it is commonly used for systems with lateral or transverse size larger than the wavelengths. That is to say that TMM is more accurate for larger cell size. Regardless of the physical size, the physical insight offered by TMM is valuable.

iii) Device simulation

As we will show in this chapter, the optical signal in a CIS is integrated to generate electrons which are transferred through the MOSFET gate to become voltage output signal. Such integration and transfer shall be modeled using the semiconductor drift-diffusion (DD) equation. The DD model solves over a mesh grid within the semiconductor the electrode potential V, as well as the carrier densities n and p.

The simulation software APSYS [3] from Crosslight is suitable for such a purpose. Please note that CIS operates in a large signal mode and transient simulation must be performed. AC analysis can be used to compute the capacitance of the output floating diffusion (FD) point. As we will show that pinned photodiode (PPD) [6] photonic integration also works in a transient mode with integrated charge proportion to the time within the proper signal cycle of the CIS system.

The APSYS simulator is the general-purpose 2D/3D finite element analysis and modeling software for semiconductor devices. All the important generation and recombination mechanisms, such as Shockley-Reed-Hall (SRH), spontaneous and Auger recombination, are taken into account. Deep trap dynamics is included for thin film solar cells. The spontaneous recombination and optical absorption can be calculated with quantum mechanics using Fermi's golden rule, which may be important for novel photosensitive devices using quantum well and quantum dot materials. The simulator solves several interwoven equations including the basic Poisson's equation, and drift-diffusion current equations for electrons and holes. Poisson's equation is as follows with Eq. (4).

$$-\nabla\cdot\left(\frac{\epsilon_0\epsilon_{dc}}{q}\nabla V\right) = -n + p + N_D(1 - f_D) - N_A f_A + \sum_j N_{tj}(\delta_j - f_{tj}), \quad (4)$$

Here the last term describes the deep trap density effect. In the above equation, V is electrical potential, ϵ_0 vacuum dielectric constant, ϵ_{dc} relative DC or low frequency dielectric constant, q electronic charge, n electron concentration, p hole concentration, N_D the shallow donor density, N_A the shallow acceptor density, f_D occupancy of the donor level, f_A occupancy of the acceptor level, N_{tj} the density of the jth deep trap, f_{tj} the occupancy of the jth deep trap level, and δ_j is 1 for donor-like traps and 0 for acceptor-like traps. The current continuity equations for electrons and holes are respectively expressed as Eq. (5) and Eq. (6), respectively,

$$\nabla \cdot J_n - \sum_j R_n^{tj} - R_{sp} - R_{st} - R_{au} + G_{opt}(t) = \frac{\partial n}{\partial t} + N_D \frac{\partial f_D}{\partial t}, \quad (5)$$

$$\nabla \cdot J_p + \sum_j R_p^{tj} + R_{sp} + R_{st} + R_{au} - G_{opt}(t) = -\frac{\partial p}{\partial t} + N_A \frac{\partial f_A}{\partial t}. \quad (6)$$

Here R_n^{tj} and R_p^{tj} are electron and hole recombination rates per unit volume through the *j*th deep trap respectively, J_n and J_p are electron and hole current flux density respectively. G_{opt} is the optic generation rate, R_{sp}, R_{st}, and R_{au} the spontaneous recombination rate, the stimulated recombination rate and the Auger recombination rate per unit volume respectively. These equations govern the electrical behavior (e.g., I-V characteristics) of a semiconductor device.

III. Physical Trend for a Simplified 2D Structure

i) Pinned photodiode with transfer gate

The basic structure of a CIS cell consists of a PPD as a photonic integrator [6], a MOSFET transfer gate (TX gate), and a reset MOSFET (RST gate). A schematic diagram is given in Fig. 1. At the heart of a CIS is the PPD for photo integration plus a transfer gate, as shown in the material structure and net-doping structure in Fig. 2. The PPD was originally designed to have n-side grounded while the p-side was designed to be floating [6]. In modern CIS design, the p-side of the PPD is heavily doped but the n-side is more likely to be connected to the source of the transfer gat. The n-side is usually lightly doped so that it acts like charge storage region.

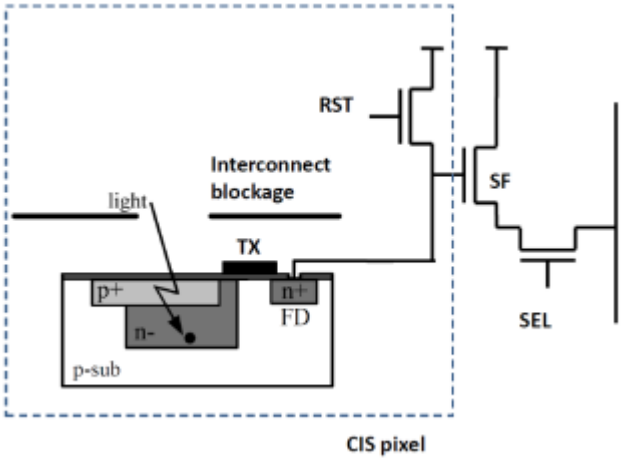

Fig. 1. Equivalent circuit diagram of a CIS.

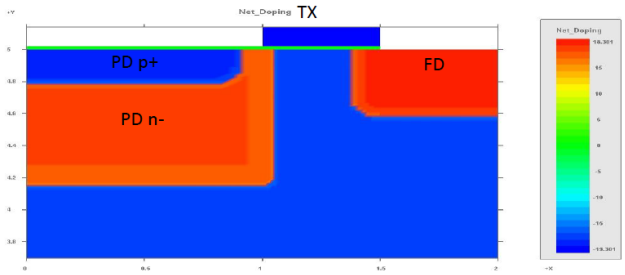

Fig. 2. Structure and net doping plot of a simplified CMOS image sensor with PPD and transfer gate.

Referring to Fig. 2, the structure has its substrate grounded and there is only one bias control contact: the MOSFET gate. The FD diffusion potential is the output of the device and it is usually connected to a source follower MOSFET which is not considered in this study. With Crosslight TCAD, a contact is automatically voltage controlled and thus we shall not define the FD output as a contact. Instead we just monitor the time dependence of a mesh point at the FD, knowing that this would be the floating voltage output to the source follower MOSFET. An alternative is to define the FD as a contact and connect it to another device with large input resistance. For AC analysis, we will use such an approach. In the meantime, we will assume the FD is an open circuit of floating voltage with its potential controlled by charge injection through the transfer MOSFET.

CIS is a photodetector and its performance is based on comparison of device response with and without light illumination. The control of various MOSFET electrodes is also an important part of CIS operation. Fig. 3 is the signal control diagram showing light illumination as one of the control parameters for this simplified CIS. The TX gate is turned on to 5 volt after a time period of the charge integration time. When doing the actual device simulation, the similar input file is run twice, one with light and one without. The light intensity for this study is set at 1000 W/m^2. For each case, we control the time variable while varying other variables such as light intensity and electrode bias.

We use the TCAD software to monitor several points of interest within the device.

- PD_pplus: top of p^+ of the PPD.
- TX_gate: channel beneath the transfer gate.
- FD: floating diffusion.
- PD_N_minus: n - side of the PPD.

It is interesting to note from Fig. 4(a) that potential at the top p^+ of PPD does not change with light during the light integration period. Its potential would increase with the TX gate when it is turned on. With light on, the carriers would cause screening of the TX gate and the increase in potential increment would be less than in the dark case.

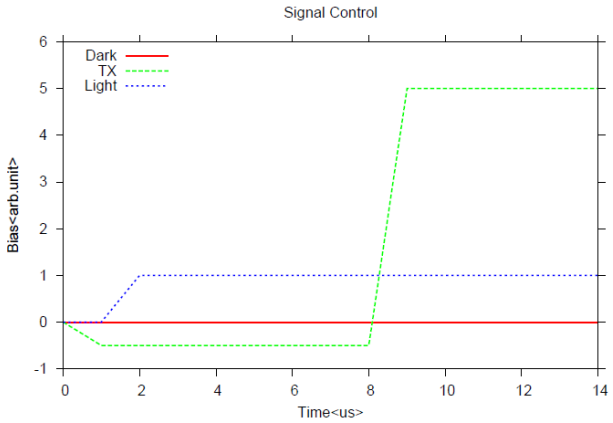

Fig. 3. Signal control for the PPD and TX gate.

It is somewhat surprising that the n-side designed to be "pinned" actually experiences a large potential swing as a result of charge integration, as indicated in Fig. 4(b). The explanation is that the n doping is much lower than the p^+ doping and thus slight change in charge distribution will cause an overall change of potential because of the large depletion width with low doping.

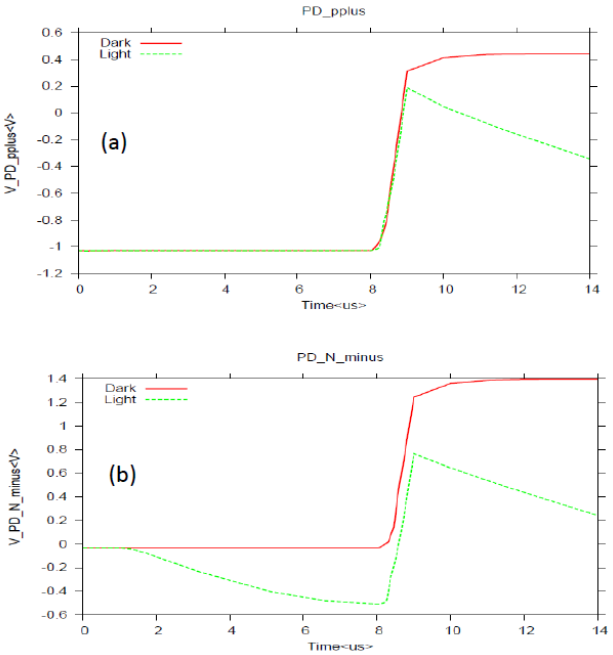

Fig. 4. (a) p^+ side potential and (b) n-side potential of the PPD as function of time.

It is important to study exactly how the PPD is collecting photon-generated carriers. We define a region near the p^+ and n- of the PD and integrate the electrons and holes there. The results are indicated in Figs. 5(a) and (b). We note that the amount of holes collected ($5x10^9$/m, unit for 2D simulation) during integration is smaller than the total amount of electron collected ($7x10^9$/m) by the n- region. The reason is that the n- region is surrounded not only by the top p^+, but it also by the p- under and around it. Some photo generated holes must have been distributed in other p regions than the top p^+ region.

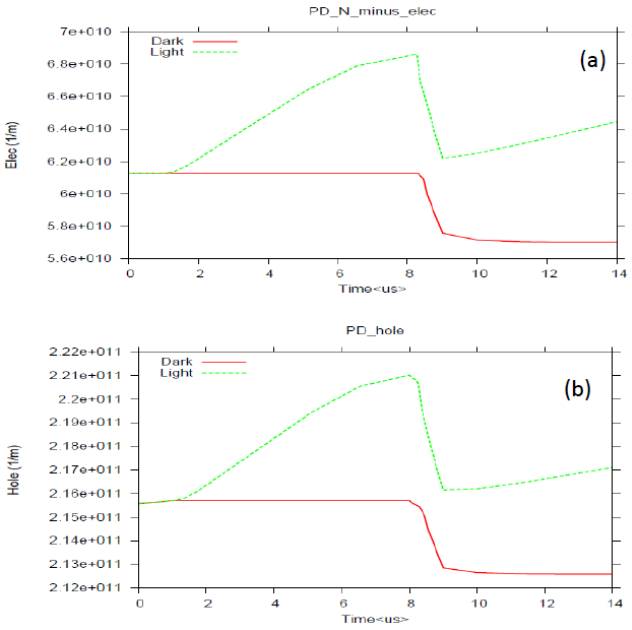

Fig. 5. (a) Integrated electron concentration near the n-side, and (b) integrated hole concentration near the p^+ side of the PD as a function of time.

The purpose of the CIS design is to transfer as many photon-generated electrons to the FD point as possible. Therefore, we integrate the FD region and count the number of electrons during the whole signal cycle for the light-illumination and dark cases. The results are shown in Fig. 6(a) which indicates approximately $3x10^9$/m electrons have been transferred from the PD at the end of the transfer period. This is approximately half of the collected photon-generated carriers in the PD. The final results of voltage output from the simplified CIS is shown in Fig. 6(b) and the potential difference between light and dark is found to be 1.2 Volt for this simple structure. The effective dynamic capacitance from transient simulation works out to be 0.4 nF/m with transferred charge given as $3x10^9$/m electrons.

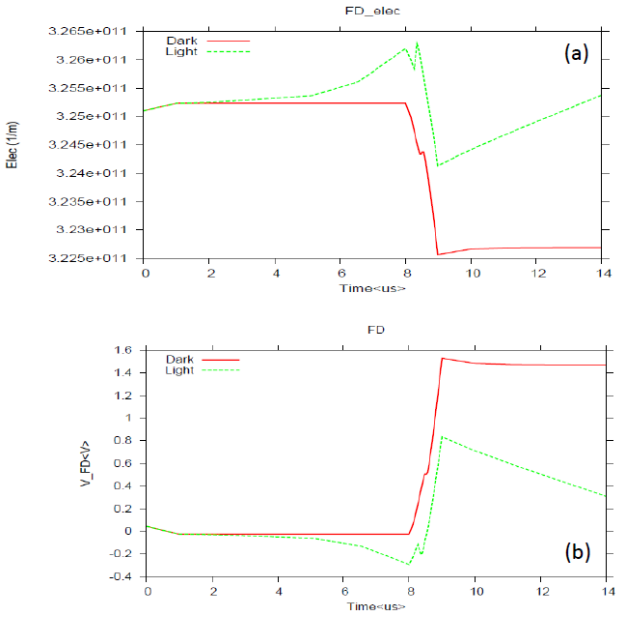

Fig. 6. (a) Integrated electron concentration around the FD region and (b) output FD voltage as a function of time.

ii) AC analysis and output capacitance

The FD output voltage is generated by injection charges. So it is natural to relate the voltage with the capacitance from the FD contact which can be measured in experiment. For computation of capacitance from APSYS, we need to create a contact (or electrode boundary) at the FD and perform an AC analysis. The AC capacitance is defined as the imaginary part of the AC current (or displacement current) induced by unit AC voltage at FD divided by angular frequency. Experimentally, it is convenient to set the measurement frequency at 1MHz.

Unfortunately for APSYS, adding a contact at FD would fix the voltage under steady state or transient conditions and it would lose the floating condition. A solution in APSYS is to attach a large resistor between the FD contact and ground. If the resistance of the resistor is sufficiently large, the FD contact will be regarded as floating.

The results of the AC analysis are shown in Figs. 7(a) and (b). It is interesting to note that carrier injection induced by light significantly reduces the capacitance of the FD contact. This can be interpreted as a carrier saturation effect: higher concentration of carriers tends to saturate the semiconductor junction and makes charge storage less responsive to voltage change. The capacitance from AC analysis is approximately 2 nF/m which is much larger than the dynamic capacitance of 0.4 nF/m. Therefore, AC analysis can be a good indication of physical trend but by no means should be regarded as a time-saving substitute of the more realistic transient simulation.

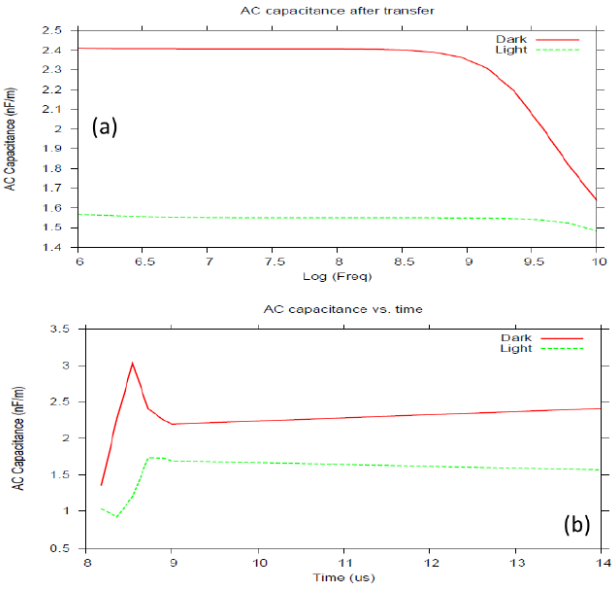

Fig. 7. (a) AC capacitance after TX transfer, and (b) dynamic output capacitance versus transient time.

iii) Traps and interface effects

Electron traps are undesirable for CIS and one of the advantages of CIS over conventional CCD is the photo integration PD is cleared of oxide/silicon interface under the MOS gate. Electrons being trapped under the gate would take time to be released and thus would cause significant background noise. The traps will also act as recombination center and thus reduce the integrated photo carriers.

The PPD is mostly away from the MOS interface but it is still being isolated by the STI or the shallow trench isolation and will still be interfaced by limited area of oxide/silicon interface. To study the effect of interface trap in this subsection, we will set the surface recombination velocity to be 1×10^6m/s for both electrons and holes on the left side interface of the CIS to mimic a STI. Here the effect is to induce recombination of photon-generated electrons and holes at the left interface and we expect reduction of photo generation.

Fig. 8(a) shows that the photo-generated electrons have been reduced by about half. Similarly, the transferred carriers and output signal are also reduced by half, as indicated in Figs. 8 (b) and 9, respectively.

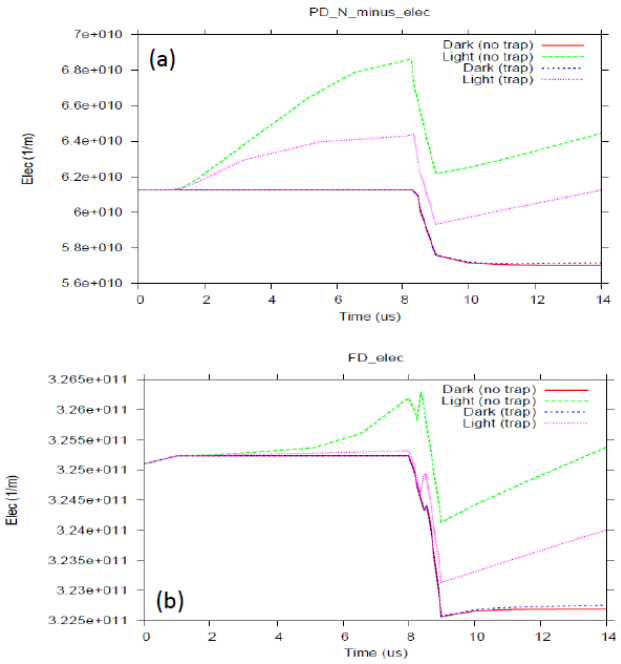

Fig. 8. Effect of interface traps as recombination centers on (a) the PD n-region, and (b) the FD region.

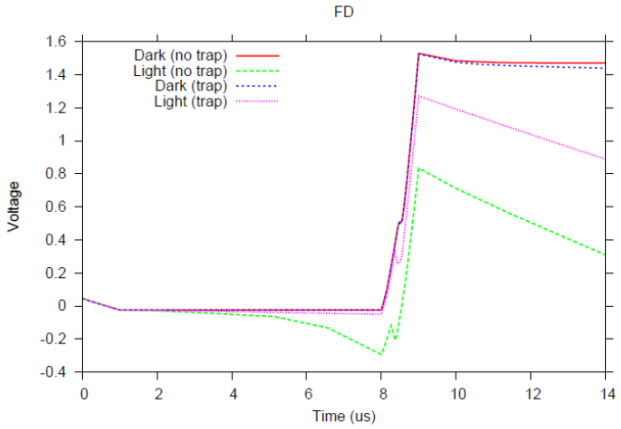

Fig. 9. Effect of interface traps as recombination centers on the output voltage at FD.

iv) CIS with transfer and reset MOSFET

A common practice is to integrate the TX and RST gate within the CIS cell for fast reset and transfer after integration. To complete our 2D simulation, we add a RST MOSFET to the right side of the previous device indicated to Fig. 2. The resulting pixel structure is shown in Fig. 10. To account for the reset process, the signal control is revised to include the reset drain and gate as indicated in Fig. 11. Since the physical models have been explained using the simplified structure, we shall only present the result of the FD in Fig. 12. We obtain much larger potential difference than the previous simplified structure in the output FD mainly because of longer integration time used for the case when there is a reset MOSET.

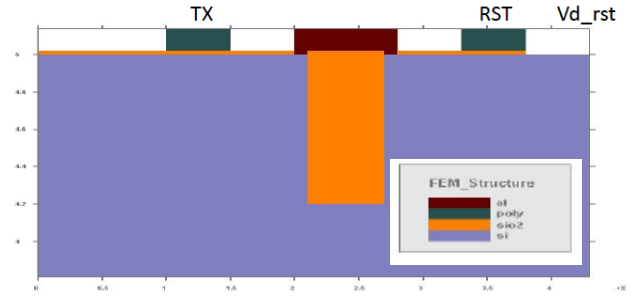

Fig. 10. CIS with PPD, TX gate & RST gate.

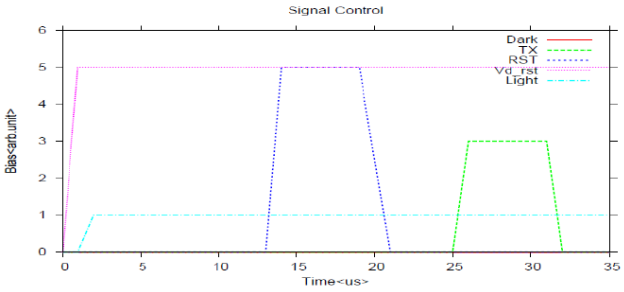

Fig. 11. Signal control diagram of a complete CIS pixel cell for 2D simulation.

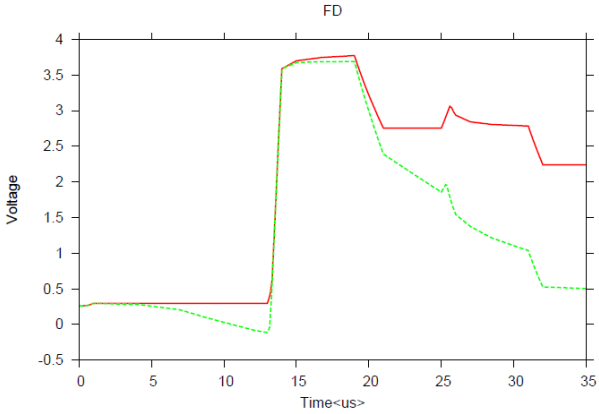

Fig. 12. FD output voltage signal of the complete 2D CIS with dark and illumination cases.

IV. 3D Simulation I: Lens and Aperture Size Effects

In this section based on Crosslight CSuprem [2] and APSYS [3] we present 3D modeling of an active pixel sensor (APS) unit and the results of process simulation and opto-electronic response performance [7-9]. Particularly

the lens and isolated metal aperture size effects will be addressed [8,9].

i) 3D APS Development by CSuprem

The schematic APS unit structure is similar to Refs. [10-13] includes a PPD, a transfer (TX) gate, and a reset (RST) gate. The whole 3D APS unit is process-built and simulated by Crosslight CSuprem with structure mesh, material together with doping information exported and interfaced to Crosslight APSYS. The Crosslight CSuprem is a process simulation software package based on the SUPREM.IV.GS code developed in Stanford University. Crosslight greatly enhanced the capability of the original code and extended it from 2D to 3D with many advanced capability and features such as ion implantation, anisotropic and sacrificial etching, deposition, diffusion, rapid thermal anneal (non-uniform temperature annealing), oxidation etc. To reduce mesh size, we assume 5-μm-thick p-type starting substrate. The detailed unit component deployment (as generated by Crosslight MaskEditor with 9 mask layers) [7-9] is schematically shown in Fig. 13. For such a simplified APS unit, the 9 major mask layers are for shallow trench isolation (STI), As implantation for n^+ region, n-type drain formation, boron implantation for p^+ photodiode, gate oxide and poly-Si formation and implantation, two contact vias, and metal layers respectively (see Appendix 1 for the Csuprem code).

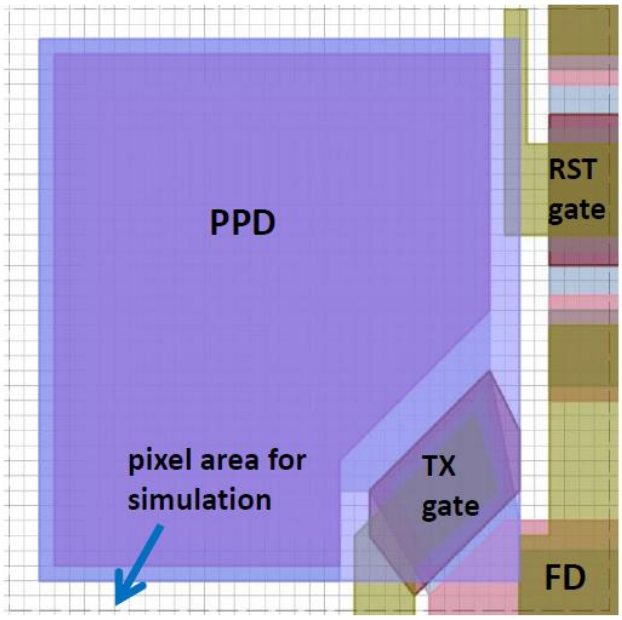

Fig. 13. Schematic APS unit deployment.

The fully process simulated structure with microlens is shown in Fig. 14 [7-9]. The 2D structure details and net doping concentration for one typical region (PPD and TX) are presented in Figs. 15 (a) and 15 (b) [7-9] respectively, and for another typical region [floating drain (FD) and RST] are presented in Figs. 16 (a) and 16 (b) [7-9] respectively.

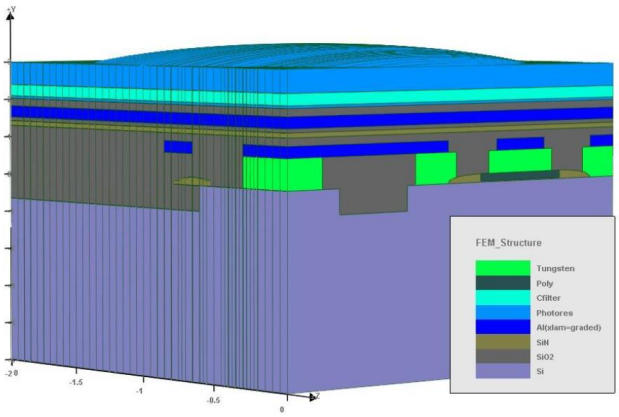

Fig. 14. 3D APS developed by CSuprem (microlens on top).

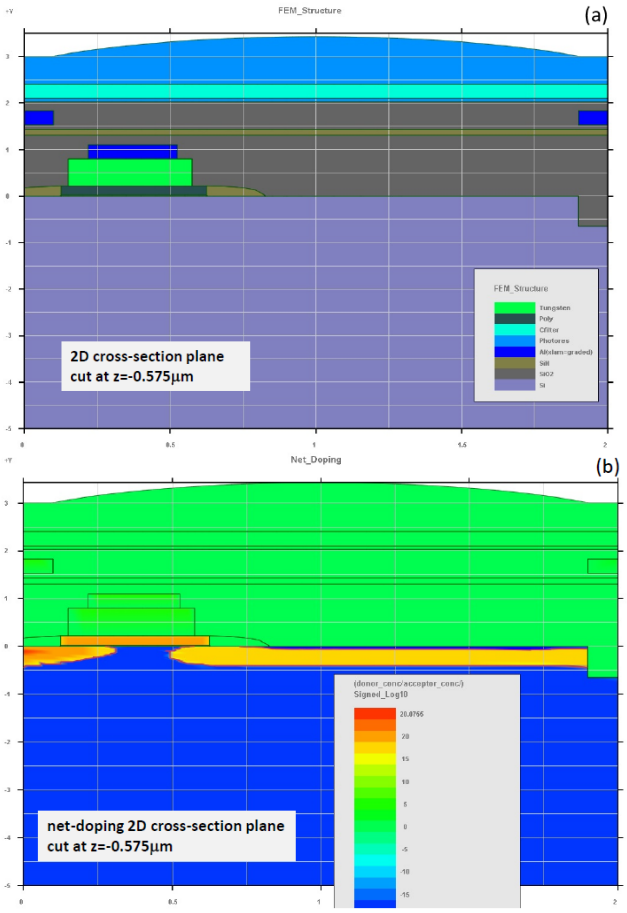

Fig. 15. (a) 2D structure details and (b) net doping concentration for one typical region (PPD and TX).

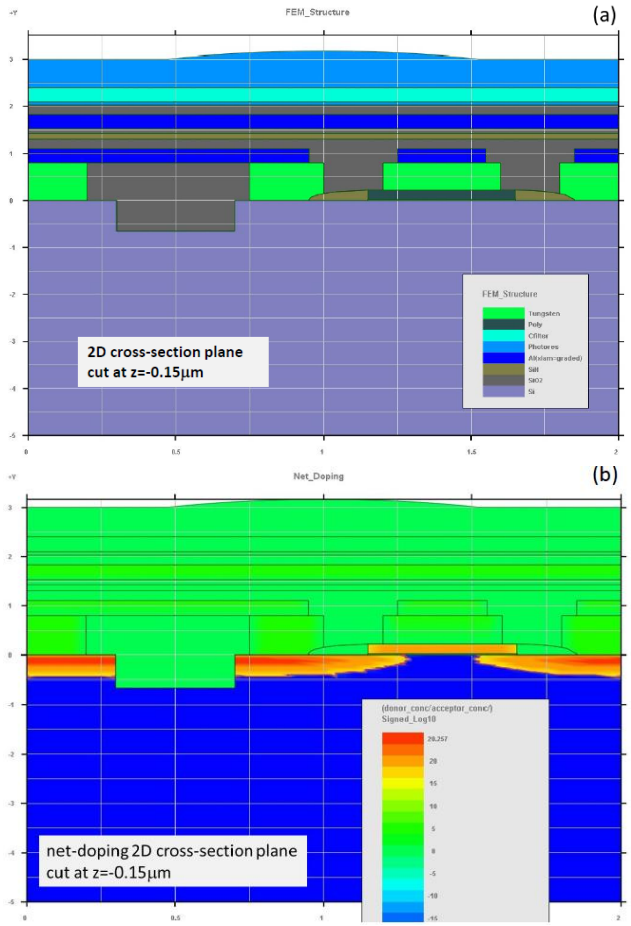

Fig. 16. (a) 2D structure details and (b) net doping concentration for another typical region (FD and RST).

ii) 3D Opto-electronic Modeling by APSYS

Taking the exported file from CSuprem, 3D modeling of opto-electronic responses is performed by using APSYS, To do FDTD, all the important material index data are converted to the coefficients of the Lorentz dispersion terms. The optical focusing effect due to the front microlens is observed with the optical energy in Fig. 17 (a) and with the propagation of the z-component electric-magnetic field in Fig. 17 (b), respectively.

For the work studied in this section, all the optical efficiency (OE) and quantum efficiency (QE) results are from FDTD simulation of the relevant CIS structures. The OE is defined as the integration of the ratio of (ingoing flux-outgoing flux)/incident flux over device interface, where ingoing flux is the difference between the incident flux and the reflected flux upon the very beginning surface illuminated first. The QE is defined as integration of (absorption rate)*(relative energy intensity) across all the device 3D grid points. The OE does not care about which material absorbs light and has electron-hole pairs generated. The QE computation involves in more mesh memory than OE but provides more insight on the photo-electric conversion efficiency than the OE.

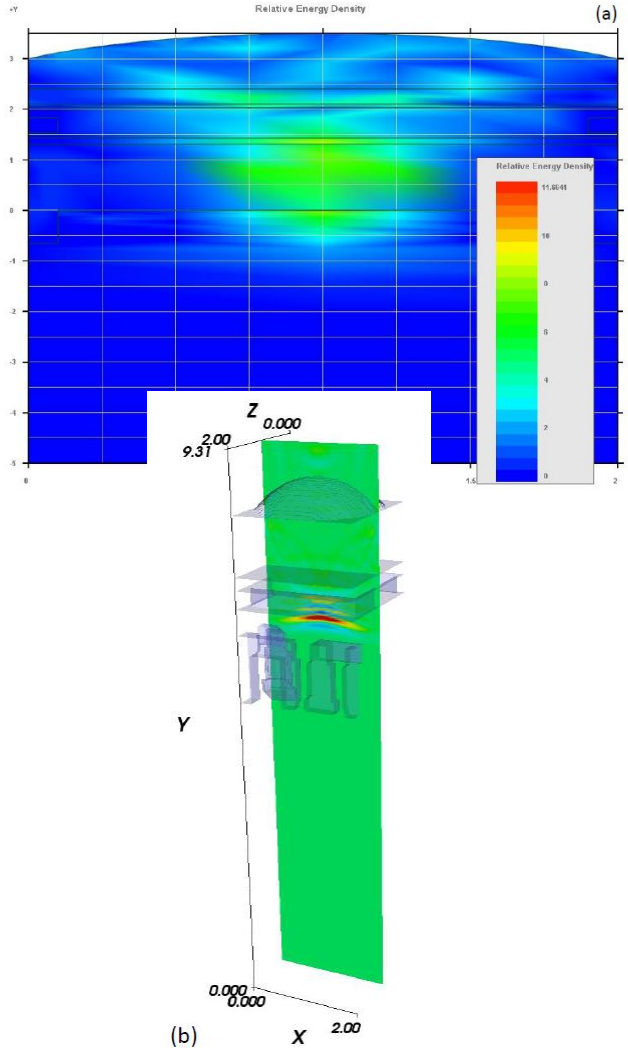

Fig. 17. (a) Focusing effect of microlens shown by 2D optic energy (cutline along z=-1.0 µm), and (b) focusing effect of microlens shown by field propagation.

With the illumination and APS unit operating bias clock shown in Fig. 18 [7-9], the evolution of the potential on FD versus time is shown in Fig. 19 [7-9]. The potential on FD above the threshold of TX gate is indeed affected by the optical power intensity whereas it is less affected before applying the RST and TX gate bias. The overshot effect from illumination can also be seen when the power intensity is very high where the potential on FD after TX stage is hardly changed as shown in Fig. 19. It is noted that

the APS read-out as experimentally demonstrated for a similar CMOS image sensor with PPD [13] shows consistency with the simulated potential evolution in Fig. 19. See Appendix 2 for APSYS simulation code for the opto-electronic response modeling.

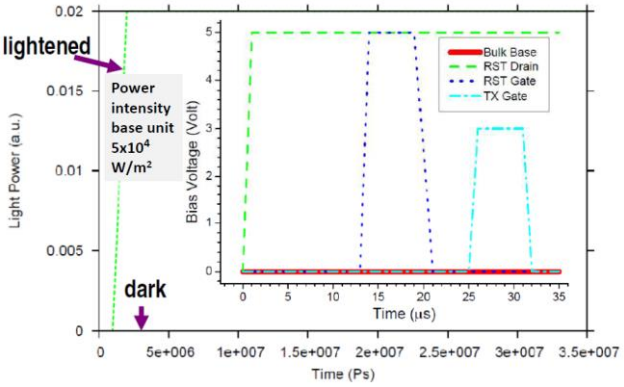

Fig. 18. Illumination and APS unit operating bias clock (inset).

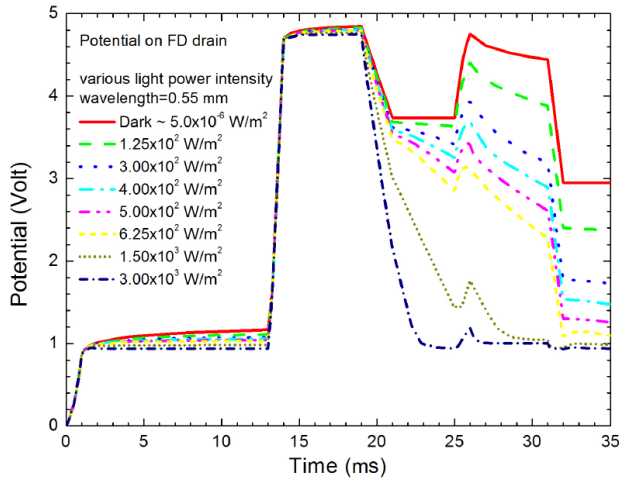

Fig. 19. Potential on FD versus time with various optical power intensity with microlens.

A flat APS unit without microlens has also been simulated for comparison. The potential difference on FD after TX stage is shown versus optical power intensity by comparing between the microlens case and flat case in Fig. 20 [7-9]. The pixel unit with microlens apparently shows improved response at relevant levels of optical power intensity. It should be noted that the microlens design must be optimized for the largest optical power intensity absorption by the PPD through a especially-designed isolation metal layer aperture as described below.

One or more metal layers are usually inserted in the PPD region of the APS structure for color isolation purposes. The opto-electronic response is also simulated versus the aperture size of this isolated metal layer in the APS structure with microlens. The potential difference on FD after TX stage is also shown in the insert of Fig. 20 [7-9] by comparing the cases of large and small apertures of isolated metal layer, respectively. The results indicate that an inappropriate aperture size for the isolated metal layer may actually lead to sensitivity loss (e.g., the small aperture case with more metal blocking). This means that metal layer deployment optimization should not be ignored for APS design consideration. Whereas more modeling work is needed on CFA and cross-talk issues [14] which involve in more mesh and computation complexity, the presented results demonstrate a methodological and technical capability for 3D modeling optimization of complex CMOS image sensor at least for a single pixel unit.

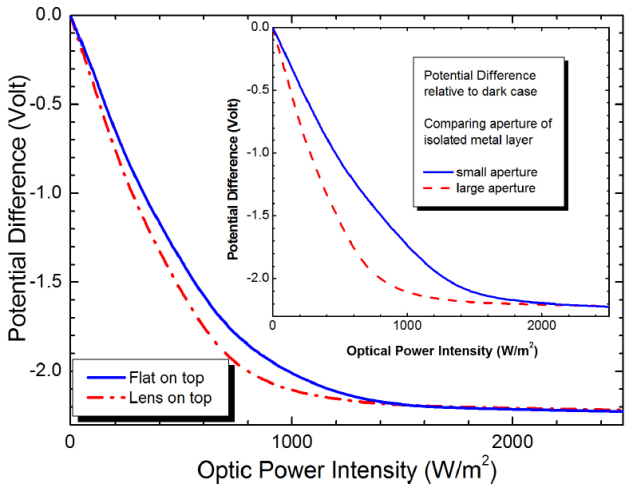

Fig. 20. Potential difference (after TX stage) versus optical power intensity comparing between flat and lens cases and (insert) comparing between small and large aperture of the isolated metal layer in the APS structure.

V. 3D Simulation II: Comparing FSI and BSI Pixels

In this section, comparison is made between front surface illumination (FSI) and back surface illumination (BSI) pixels [15-17], which are built by Crosslight LayerBuilder and simulated by APSYS [3] and OptoWizard [4], will be comparatively presented [17].

The 3D CIS structures could be simply formed by Crosslight LayerBuilder with multi-layers/columns by taking the advantage of the 3D-connect flow option. The

schematic APS unit structure is similar to Ref. [7-13] including a pinned photodiode, a transfer (TX) gate, and a reset (RST) gate. Due to the thinning request and also to reduce the mesh size, we assume 5-μm-thick p-type starting substrate. The typical CIS schematic (regular geometry) with Crosslight LayerBuilder only is shown in Fig. 21 (a) [17]. These two structures with 3D connect-flow are shown in Fig. 21 (b) and (c) for FSI and BSI with color filter array (CFA), respectively. Trench insulators are inserted among PPD, TX gate and RST gate. Most of the front surface is simply assumed to be covered with thin SiO2 as anti-reflection coating layer whereas the back surface is the (thinned) wafer base. The CFA is included on the top and at the bottom of the structure as shown on Fig. 21 (b) and (c), respectively.

The operating illumination and bias time clock cycle (reset at first and then transfer) is still assumed to be the same as in Refs [7-9], as shown in Fig. 18. The evolution of the potential on the floating drain (FD) versus time is shown in Fig. 22 (a) and (b) respectively for FSI and BSI pixel, respectively. With increasing power intensity, the potential on FD shows increasingly large difference relative to the dark case at the transfer stage, similar to Fig. 19. When the power intensity reaches certain level, the overshot-effect becomes dominant at the transfer stage. Although not presented here, the results during the modeling process also indicate a 3D current crowding effect, leading to poor sensitivity. This is shown by small or unchanged potential difference relative to the dark case at the transfer stage at appropriate optical power intensity of illumination when a too-wide PPD range is set along the transfer gate and with poor trench insulation.

The potential difference (relative to dark case) on the FD after transfer stage (the end of the time evolution cycle) versus optical power intensity is shown in Fig. 23 (a) for BSI and FSI pixels by comparison at 0.55-μm wavelength. The BSI pixel shows larger potential difference indicating improved sensitivity than the FSI pixel. The improved sensitivity with BSI is also observed with the potential difference versus wavelength plots for both FSI and BSI cases as shown in Fig. 23 (b) [17] with a comparison. It should be noted of that the results shown are based on the simple material structures as shown in Fig. 21 (b) and (c). Complicated wavelength dependency might be expected when more materials are involved in the pixel buildup.

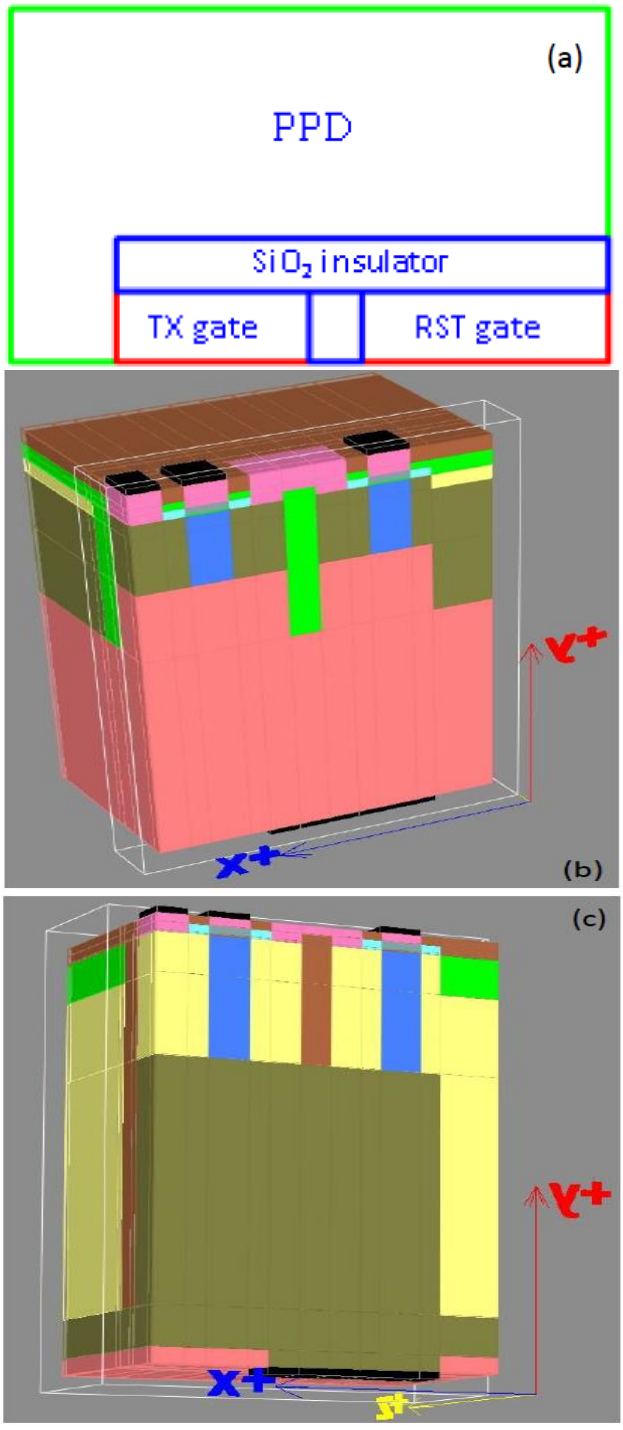

Fig. 21. (a) Typical schematic APS unit deployment (regular geometry) [17], (b) 3D FSI with CFA, and (c) 3D BSI pixel structures with CFA built by Crosslight LayerBuilder.

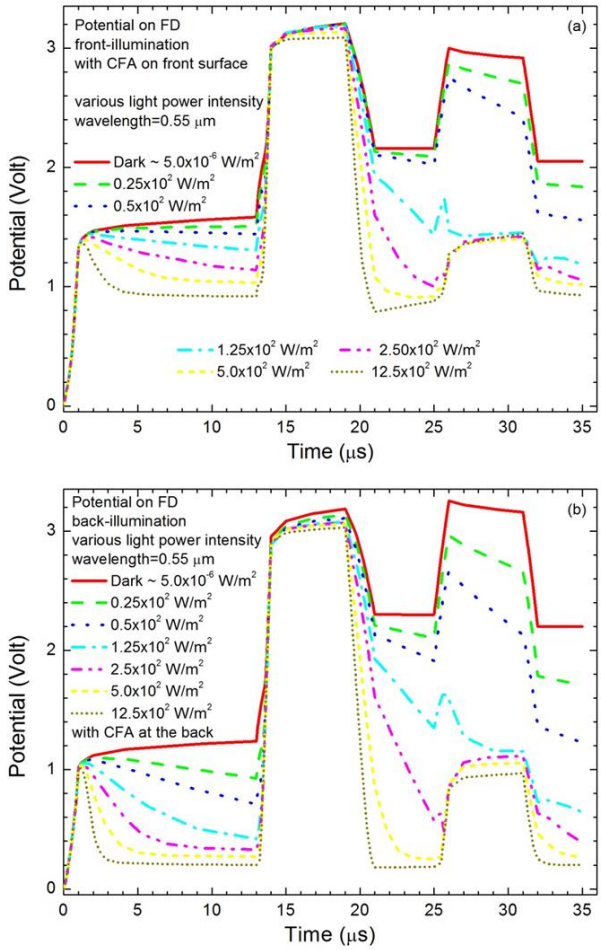

Fig. 22. Potential evolution versus time on FD for (a) FSI and (b) BSI pixels with CFA.

Since the previous opto-electronic results support the BSI pixel design, it might be interesting to look at a purely optical perspective using the results from FDTD. In Fig. 24 (a) and (b) [17], respectively, the OE and QE results are compared between the BSI and FSI cases. Although the accuracy of FDTD simulation relies on large memory mesh with detailed and correct compilation of various material dispersion profiles, the results, especially the QE ones, indicate that the BSI pixel shows better sensitivity than the FSI pixel at least within certain wavelength range for the pixel structures studied in this work, especially when full dispersion profiles for all the involved materials are considered for the FDTD computation. The QE results are consistent with the opto-electronic response results presented in Fig. 23 (b). It is noted of that the OE results present high value throughout most of the main wavelength range and do not show the same trend as the QE results. This is because that the definition of OE is "how much flux is absorbed in device regardless of material distribution" and the CFA is highly absorptive. On the other hand, QE counts number of photo-generated carriers only in the silicon region. So, QE results should provide more reliable insight on the pixel performance. See Appendix 3 for QE modeling of BSI pixel by FDTD with Crosslight CLFDTD and OptoWizard [5].

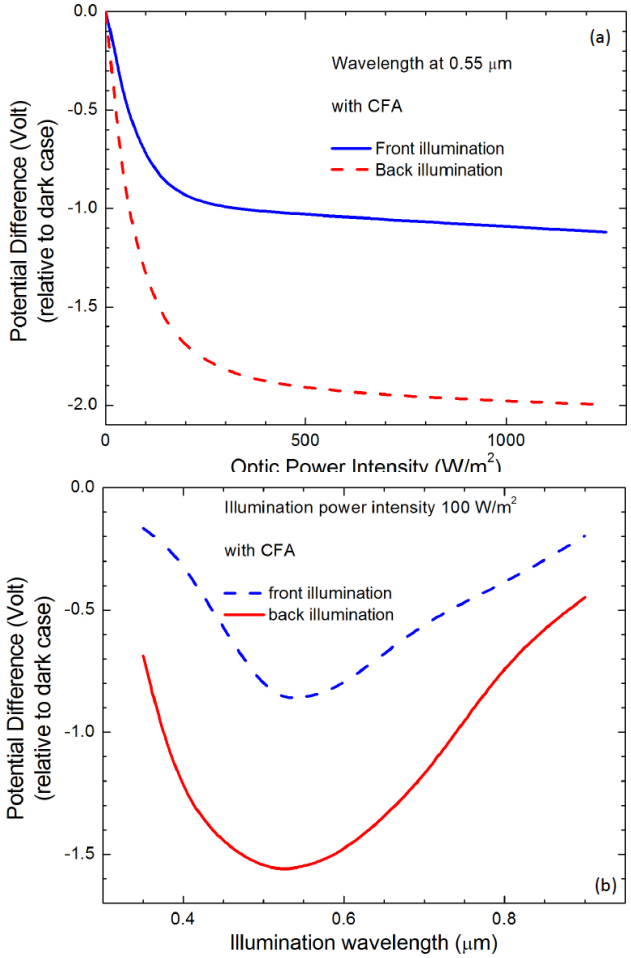

Fig. 23. (a) Potential difference (at the end of TX stage with illumination at 0.55 μm) versus optical power intensity, and (b) potential difference (at the end of TX stage) vs. wavelength, comparing between FSI and BSI pixels with CFA.

Under some circumstances during our simulation, the BSI pixel still shows better sensitivity of charge transfer as with potential difference change than the FSI pixel even though the BSI pixel has lower OE (or/and even lower QE) near the peak wavelength range than the FSI pixel. This prompts us to conclude that, for CIS, modeling solely based on optical OE and QE may not be enough to judge the actual pixel performance. The sensitivity is better represented by the potential difference with opto-electronic response as the OE or even the QE lacks the

modeling mechanism for the charge-voltage conversion in the pixel [15]. This drives the need for the TCAD suite with a full breadth of highly integrated process, optical and electronic modeling for CIS design and optimization.

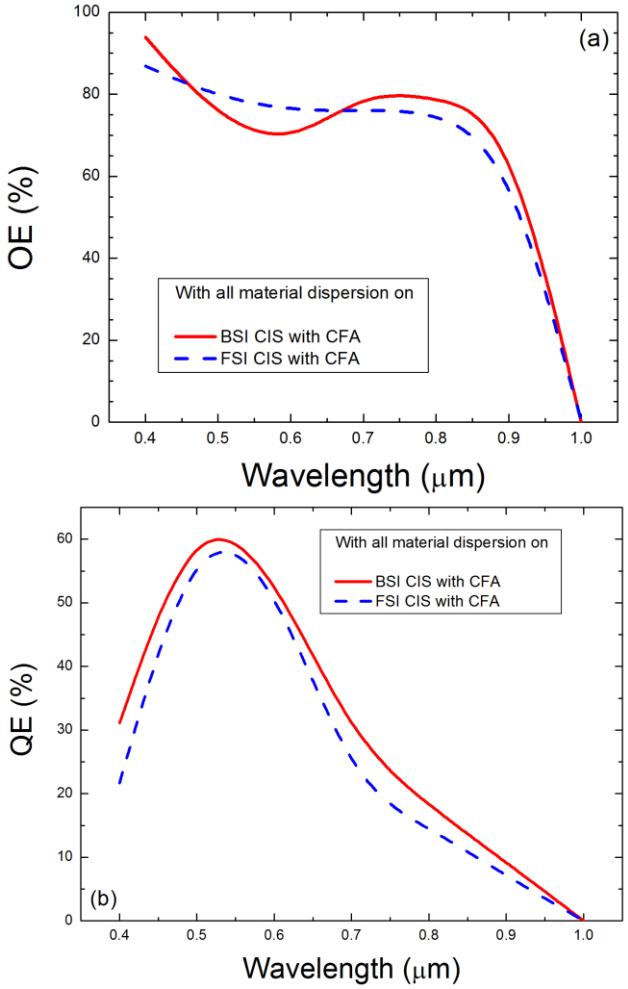

Fig. 24. Optical FDTD simulation results of (a) OE and (b) QE comparison between FSI and BSI pixels with CFA.

More optimization work is apparently needed on improved CFA design, the structure layout optimization together with the combined opto-electronic simulation. Further work relevant to CFA is cross-talk issues between (among) neighboring pixels. This would involve in more mesh and computation complexity.

VI. Summary

TCAD simulation of CMOS active pixel image sensor from process to opto-electronic response is presented in this application note with a full suite of modeling software developed by Crosslight. The opto-electronic responses are presented versus various power intensity, illumination wavelength, and aperture size effect together with some OE/QE results. It shows that CIS design strongly depends on the interaction of optical and electrical effects. It indicates that accurate simulation requires a full suite of 3D TCAD software capable for process, optics and device simulations. The results demonstrate a methodological and technical capability by using Crosslight software for 3D modeling optimization of complex CMOS image sensor.

References

1. marketsandmarkets.com, "Image Sensor Market by Type (CMOS, CCD, and Others), Specification, Application (Aerospace, Automotive, Consumer Electronics, Healthcare, Industrial, Entertainment, and Security & Surveillance), and Region -Global Forecast to 2020," Publishing Date: October 2015, Report Code: SE 2676, http://www.marketsandmarkets.com/Market-Reports/ImageSensor-Semiconductor-Market-601.html

2. Crosslight Software Inc., CSuprem, Process simulation of semiconductors, http://www.crosslight.com

3. Crosslight Software Inc., APSYS, Advanced Physical Simulation Software for Semiconductor Devices http://www.crosslight.com

4. Crosslight Software Inc., OPTOWIZARD, Advanced Optical Field Analysis Software http://www.crosslight.com

5. Li, S., and Y. Fu 2011. 3D TCAD Simulation for Semiconductor Processes, Devices and Optoelectronics. Springer.

6. Weckler, G. P. 1967. Operation of p-n junction photodtectors in a photon flux integrating mode. IEEE J. Solid-State Circuits 2:65-73.

7. Li, Z. M. S., Y.G. Xiao, K. Uehara, M. Lestrade, S. Gao, Y. Fu, Z. Q. Li, and Y.J. Zhou 2011. 3D modeling of CMOS image sensor: from process to opto-electronic response. Paper presented at the 2011 International Conference of Electron Devices and Solid-State Circuits (EDSSC 2011) (2 pages).

8. Xiao, Y. G., Z. M. S. Li, K. Uehara, M. Lestrade, and Z. Q. Li 2011. 3D modeling of active pixel sensor with microlens. Paper presented at the 17th Microoptics Conference (MOC' 1 1) (2 pages).

9. Li, Z. M. S., Y. G. Xiao, K. Uehara, M. Lestrade, S. Gao, Y. Fu, Z.Q. Li, and Y.J. Zhou 2013. 3D modeling of CMOS image sensor and aperture size effect. Paper presented at the NUSOD 2013. 125-126.

10. Fossum, E. R. 1997. CMOS image sensors: Electronic camera on a chip. IEEE Trans. Electron. Dev. 44:1689-1698.

11 Fossum, E. R., and D. B. Hondongwa 2014. A review of the pinned photodiode for CCD and CMOS image sensors. IEEE J. Electron Dev. Sci. 2:33-43.

12. Bigas, M., E. Cabruja, J. Forest, and J. Salvi 2006. Review of CMOS image sensors. Microelectron. Journal 37:433-451.

13. Cho, Y.-S., H.Takao, K. Sawada, M. Ishida, and S.-Y. Choi 2007. High speed SOI CMOS image sensor with pinned photodiode on handle wafer. Microelectron. Journal 38:102-107.

14. Fesenmaier, C. C., Y. Huo and P. B. Catrysse 2008. Optical confinement methods for continued scaling of CMOS image sensor pixels. Optical Express 16:20457-70.

15. Arai, T., and H. Shimamoto 2014. Simulation-based design of a pixel for back-side-illuminated CMOS image sensor with thick photo-electric conversion element. Proc SPIE 8982:898227-1-9.

16. Xiao, Y. G., K. Uehara, S. Gao, Y. Fu, M. Lestrade, Z. Q. Li, Y. J. Zhou, and Z. M. S. Li 2015. 3D modeling of CMOS image sensor: comparison between front- and back-illumination. Paper presented at NUSOD 2015. 175-176.

17. Xiao, Y. G., K. Uehara, Y. Fu, M. Lestrade, Z. Q. Li, Y. J. Zhou, and Z. M. S. Li 2016. Toward designing back-illuminated CMOS image sensor based on 3D modeling. Paper presented at the Photonics West 2016 (8 pages).

Appendix

Appendix_1: CSuprem simulation code to generate the 3D CIS with microlens

```
#option bar
mode quasi3d
#mode three.dim
#mater_define material_label=photoresist macro_name=photores
mater_define material_label=tungsten mater_lib=Tungsten
mater_define material_label=CFA mater_lib=Cfilter
option auto.mesh.implant=false
#
3d_mesh nsegm=66 inf=geo
# for 3D, restart after loading 3d mesh
#restart file=38_2ndph.str
#option stanford_implant_table=false
init boron conc=5.0e16
struct outf=01_sub.str
#
# --------> 3D- STI
include file=cis_cut1.msk
struct outf=02_sti_etch.str
#
deposit oxide thick=0.7
struct outf=03_sti_fill.str
#
foreach %zk (1 to 66 step 1)
etch start x=-1 y=-2 segm=%zk
etch conti x=-1 y=0. segm=%zk
etch conti x=4. y=0.  segm=%zk
etch done  x=4. y=-2  segm=%zk
end
#
struct outf=04_sti_cmp.str
#
# -------->end 3D- STI
#
deposit oxide thick=0.005
include file=cis_cut2.msk
struct outf=05_PDn_mask.str
#
implant ars energy=400 dose=1e13 angle=0 rot=0
implant ars energy=320 dose=1e13 angle=0 rot=0
implant ars energy=240 dose=1e13 angle=0 rot=0
implant ars energy=100 dose=1e13 angle=0 rot=0
#
foreach %zk (1 to 66 step 1)
etch photoresist all segm=%zk
end
#
foreach %zk (1 to 66 step 1)
etch start x=-1 y=-2 segm=%zk
etch conti x=-1 y=0. segm=%zk
etch conti x=4. y=0.  segm=%zk
etch done  x=4. y=-2  segm=%zk
end
#
struct outf=06_PDn.str
#
diffuse time=30 temp=1000
#regrid refine=true
#
struct outf=07_PDn_doping.str
#
deposit oxide thick=0.009
```

```
include file=cis_cut3.msk
struct outf=08_Drain_mask.str
#
implant ars energy=180 dose=5e15 angle=0 rot=0
implant ars energy=100 dose=1e15 angle=0 rot=0
implant ars energy=60 dose=1e14 angle=0 rot=0
#
foreach %zk (1 to 66 step 1)
etch photoresist all segm=%zk
end

foreach %zk (1 to 66 step 1)
etch start x=-1 y=-2 segm=%zk
etch conti x=-1 y=0. segm=%zk
etch conti x=4. y=0. segm=%zk
etch done  x=4. y=-2 segm=%zk
end
#
struct outf=09_Drain.str
#
diffuse time=15 temp=1000
struct outf=10_Drain_doping.str
##
deposit oxide thick=0.009
include file=cis_cut4.msk
struct outf=11_PDp_mask.str
#
implant boron energy=4 dose=3.0e13 angle=0 rot=0
#
foreach %zk (1 to 66 step 1)
etch photoresist all segm=%zk
end
#
foreach %zk (1 to 66 step 1)
etch start x=-1 y=-2 segm=%zk
etch conti x=-1 y=0. segm=%zk
etch conti x=4. y=0.  segm=%zk
etch done  x=4. y=-2  segm=%zk
end
struct outf=12_PDp.str
#
#regrid refine=true
diffuse time=3 temp=1000
#
struct outf=13_PDp_doping.str
#
# === Use a simple mosfet process here
#deposit oxide thick=0.005
deposit oxide thick=0.02 meshlayer=10
struct outf=14_mosfet_gateoxide.str
include file=cis_cut5.msk
struct outf=15_mosfet_gateoxide.str
#
#deposit the gate poly
deposit poly thick=0.2 meshlayer=4 phos conc=1.0e19
struct outf=16_mosfet_poly.str
include file=cis_cut6.msk
struct outf=17_mosfet_poly.str
#
##anneal
diffuse time=3 temp=1000
struct outf=18_mosfet_polyanneal.str
#
deposit nitride thick=0.2 space=0.05
foreach %zk (1 to 66 step 1)
```

```
etch nitride dry thick=0.2 segm=%zk
end
###################################
regrid log10.change=12.0 refine
###################################
struct outf=19_SiN_passivation.str
#
deposit oxide thick=0.8
struct outf=19A_Oxide_passivation.str
#
foreach %zk (1 to 66 step 1)
etch start x=-1 y=-2 segm=%zk
etch conti x=-1 y=-0.8 segm=%zk
etch conti x=4. y=-0.8 segm=%zk
etch done  x=4. y=-2 segm=%zk
end
struct outf=20_after_passivation.str
#
option etch.type=2
#
include file=cis_cut7.msk
struct outf=22_VIA_hole.str
#
# deposit tungsten
deposit tungsten thick=0.8 meshlayer=3
struct outf=23_VIA_deposit.str
#
foreach %zk (1 to 66 step 1)
etch start x=-1 y=-2 segm=%zk
etch conti x=-1 y=-0.8 segm=%zk
etch conti x=4. y=-0.8  segm=%zk
etch done  x=4. y=-2  segm=%zk
end
#
struct outf=24_VIA.str
#
deposit oxide thick=0.3
struct outf=29_pre_metal.str
#
include file=cis_cut8.msk
struct outf=30_metal_hole.str
#
# deposit metal
deposit alum thick=0.3 meshlayer=3
struct outf=31_metal_deposit.str
#
foreach %zk (1 to 66 step 1)
etch start x=-1 y=-2 segm=%zk
etch conti x=-1 y=-1.1 segm=%zk
etch conti x=4. y=-1.1  segm=%zk
etch done  x=4. y=-2  segm=%zk
end
#
struct outf=32_metal.str
#
#regrid log10.change=5.0 refine
#
deposit oxide thick=0.2050
struct outf=33_dpst01.str
deposit nitride thick=0.1250
struct outf=34_dpst02.str
deposit oxide thick=0.4000
struct outf=35_dpst03.str
#
include file=cis_cut9.msk
```

```
struct outf=35_metal2_hole.str
# deposit metal
deposit alum thick=0.4 meshlayer=3
struct outf=35_metal_deposit.str
#
foreach %zk (1 to 66 step 1)
etch start x=-1 y=-2.5 segm=%zk
etch conti x=-1 y=-1.83 segm=%zk
etch conti x=4. y=-1.83  segm=%zk
etch done  x=4. y=-2.5  segm=%zk
end
#
struct outf=35_metal.str
#
deposit oxide thick=0.2
struct outf=35_oxide.str
#
deposit photoresist thick=0.0700
struct outf=36_1stph.str
# Deposit color filter material
deposit CFA thick=0.3 meshlayer=2
struct outf=37_CFA.str
deposit photoresist thick=0.2
struct outf=38_2ndph.str
deposit photoresist thick=0.9 meshlayer=3
struct outf=39_ph_bf_lense.str
#
# making lens
include file=make_lens.txt
struct outf=40_final.str
#
export outfile=sup.aps xpsize=0.001
quit
```

Appendix 2: APSYS opto-electronic response simulation of the 3D CIS with micro lens

```
begin
use_macrofile macro1=my.mac
include file=zmesh.zst &&
  ignore1=load_mesh ignore2=output ignore3=export_3dgeo
load_mesh mesh_inf=sup.aps  suprem_import=yes suprem_cpl_import=no
output sol_outf=PIVnnc.out
$
more_bias_output variable=potential near_xyz=(1.0 0.0 -1.0)
more_bias_output variable=potential near_xyz=(0.35 1.1 -0.55)
more_bias_output variable=potential near_xyz=(0.15 1.1 -0.15)
more_bias_output variable=potential near_xyz=(0.85 1.1 -0.15)
more_bias_output variable=potential near_xyz=(1.4 1.1 -0.15)
more_bias_output variable=potential near_xyz=(1.9 1.1 -0.15)
$
more_output space_charge=yes
$
suprem_to_apsys_material suprem_mater=3  apsys_mater=1
suprem_to_apsys_material suprem_mater=1  apsys_mater=2
suprem_to_apsys_material suprem_mater=2  apsys_mater=3
suprem_to_apsys_material suprem_mater=6  apsys_mater=4
suprem_to_apsys_material suprem_mater=7  apsys_mater=5
suprem_to_apsys_material suprem_mater=79  apsys_mater=6
suprem_to_apsys_material suprem_mater=4  apsys_mater=7
suprem_to_apsys_material suprem_mater=78  apsys_mater=8
$
```

```
begin_zmater zseg_num=1
suprem_property user_material_mapping = yes
material_label_define label=Si mater=   1
material_lib name=Si mater=   1
material_label_define label=SiO2 mater=   2
material_lib name=SiO2 mater=   2
material_label_define label=SiN mater=   3
material_lib name=SiN mater=   3
material_label_define label=Al mater=   4
material_lib name=Al mater=   4 &&
  var_symbol1=xlam  var1=  0.5500E+00
material_label_define label=Photores mater=   5
material_lib name=Photores mater=   5
material_label_define label=CFA mater=   6
material_lib name=Cfilter mater=   6
light_power light_dir=top wavelength=0.55 incident_power=5.0e4
impact_chynoweth elec_set1=(7.03e7 1.231e8 1) &&
  hole_set1=(1.582e8 2.036e8 1) elec_setnum=1 &&
  hole_setnum=1 mater=1
end_zmater
start_loop symbol=%zk value_from=2 value_to=30 step=1
begin_zmater  zseg_num=%zk
  suprem_property user_material_mapping = yes
  define_material mater=1
  define_material mater=2
  define_material mater=3
  define_material mater=4
  define_material mater=5
  define_material mater=6
  light_power light_dir=top wavelength=0.55 incident_power=5.0e4
  impact_chynoweth elec_set1=(7.03e7 1.231e8 1) &&
      hole_set1=(1.582e8 2.036e8 1) elec_setnum=1 &&
      hole_setnum=1 mater=1
  suprem_contact num=4 xrange=(0.1 1.9) side=lower touch_mater=1
  contact num=4
end_zmater
end_loop
begin_zmater  zseg_num=31
  suprem_property user_material_mapping = yes
  define_material mater=1
  define_material mater=2
  define_material mater=3
  define_material mater=4
  define_material mater=5
  define_material mater=6
  material_label_define label=Poly mater=   7
  material_lib name=Poly mater=   7
  light_power light_dir=top wavelength=0.55 incident_power=5.0e4
  impact_chynoweth elec_set1=(7.03e7 1.231e8 1) &&
      hole_set1=(1.582e8 2.036e8 1) elec_setnum=1 &&
      hole_setnum=1 mater=1
  suprem_contact num=4 xrange=(0.1 1.9) side=lower touch_mater=1
  contact num=4
end_zmater
start_loop symbol=%zk value_from=32 value_to=34 step=1
begin_zmater  zseg_num=%zk
suprem_property user_material_mapping = yes
define_material mater=1
define_material mater=2
define_material mater=3
define_material mater=4
define_material mater=5
define_material mater=6
define_material mater=7
light_power light_dir=top wavelength=0.55 incident_power=5.0e4
```

```
  impact_chynoweth elec_set1=(7.03e7 1.231e8 1) &&
      hole_set1=(1.582e8 2.036e8 1) elec_setnum=1 &&
      hole_setnum=1 mater=1
  suprem_contact num=4 xrange=(0.1 1.9) side=lower touch_mater=1
  contact num=4
end_zmater
end_loop
begin_zmater  zseg_num=35
  suprem_property user_material_mapping=yes
  define_material mater=1
  define_material mater=2
  define_material mater=3
  define_material mater=4
  define_material mater=5
  define_material mater=6
  define_material mater=7
  material_label_define label=tungsten mater=   8
  material_lib name=Tungsten mater=   8
  light_power light_dir=top wavelength=0.55 incident_power=5.0e4
  impact_chynoweth elec_set1=(7.03e7 1.231e8 1) &&
      hole_set1=(1.582e8 2.036e8 1) elec_setnum=1 &&
      hole_setnum=1 mater=1
  suprem_contact num=4 xrange=(0.1 1.9) side=lower touch_mater=1
  contact num=4
end_zmater
start_loop symbol=%zk value_from=36 value_to=38 step=1
begin_zmater  zseg_num=%zk
  suprem_property user_material_mapping = yes
  define_material mater=1
  define_material mater=2
  define_material mater=3
  define_material mater=4
  define_material mater=5
  define_material mater=6
  define_material mater=7
  define_material mater=8
  light_power light_dir=top wavelength=0.55 incident_power=5.0e4
  impact_chynoweth elec_set1=(7.03e7 1.231e8 1) &&
      hole_set1=(1.582e8 2.036e8 1) elec_setnum=1 &&
      hole_setnum=1 mater=1
  suprem_contact num=4 xrange=(0.1 1.9) side=lower touch_mater=1
  contact num=4
end_zmater
end_loop
start_loop symbol=%zk value_from=39 value_to=47 step=1
begin_zmater  zseg_num=%zk
  suprem_property user_material_mapping=yes
  define_material mater=1
  define_material mater=2
  define_material mater=3
  define_material mater=4
  define_material mater=5
  define_material mater=6
  define_material mater=7
  define_material mater=8
  light_power light_dir=top wavelength=0.55 incident_power=5.0e4
  impact_chynoweth elec_set1=(7.03e7 1.231e8 1) &&
      hole_set1=(1.582e8 2.036e8 1) elec_setnum=1 &&
      hole_setnum=1 mater=1
  suprem_contact num=1 xrange=(0.2 0.65) yrange=(0.7 1.3) &&
      side=within touch_mater=4
  contact num=1
  suprem_contact num=4 xrange=(0.1 1.9) side=lower touch_mater=1
  contact num=4
end_zmater
```

```
end_loop
start_loop symbol=%zk value_from=48 value_to=50 step=1
begin_zmater  zseg_num=%zk
  suprem_property user_material_mapping = yes
  define_material mater=1
  define_material mater=2
  define_material mater=3
  define_material mater=4
  define_material mater=5
  define_material mater=7
  define_material mater=8
  light_power light_dir=top wavelength=0.55 incident_power=5.0e4
  impact_chynoweth elec_set1=(7.03e7 1.231e8 1) &&
      hole_set1=(1.582e8 2.036e8 1) elec_setnum=1 &&
      hole_setnum=1 mater=1
end_zmater
end_loop
start_loop symbol=%zk value_from=51 value_to=54 step=1
begin_zmater  zseg_num=%zk
  suprem_property user_material_mapping = yes
  define_material mater=1
  define_material mater=2
  define_material mater=3
  define_material mater=4
  define_material mater=5
  define_material mater=6
  define_material mater=7
  light_power light_dir=top wavelength=0.55 incident_power=5.0e4
  impact_chynoweth elec_set1=(7.03e7 1.231e8 1) &&
      hole_set1=(1.582e8 2.036e8 1) elec_setnum=1 &&
      hole_setnum=1 mater=1
end_zmater
end_loop
start_loop symbol=%zk value_from=55 value_to=61 step=1
begin_zmater  zseg_num=%zk
  suprem_property user_material_mapping = yes
  define_material mater=1
  define_material mater=2
  define_material mater=3
  define_material mater=4
  define_material mater=5
  define_material mater=6
  define_material mater=8
  light_power light_dir=top wavelength=0.55 incident_power=5.0e4
  impact_chynoweth elec_set1=(7.03e7 1.231e8 1) &&
      hole_set1=(1.582e8 2.036e8 1) elec_setnum=1 &&
      hole_setnum=1 mater=1
end_zmater
end_loop
start_loop symbol=%zk value_from=62 value_to=66 step=1
begin_zmater  zseg_num=%zk
  suprem_property user_material_mapping = yes
  define_material mater=1
  define_material mater=2
  define_material mater=3
  define_material mater=4
  define_material mater=5
  define_material mater=6
  define_material mater=7
  define_material mater=8
  light_power light_dir=top wavelength=0.55 incident_power=5.0e4
  impact_chynoweth elec_set1=(7.03e7 1.231e8 1) &&
      hole_set1=(1.582e8 2.036e8 1) elec_setnum=1 &&
      hole_setnum=1 mater=1
  suprem_contact num=2 xrange=(1.25 1.55) yrange=(0.7 1.3) &&
```

```
        side=within touch_mater=4
  contact num=2
  suprem_contact num=3 xrange=(1.85 2.0) yrange=(0.7 1.3) &&
        side=within touch_mater=4
  contact num=3
end_zmater
end_loop
$
$$--------------------------
$$ Setting for MEEP(FDTD)
$$--------------------------
$$ position and size of light source
fdtd_source component=Ex  &&
  center=(1.0 8.7 1.0) size = (2.0 0.0 2.0)
fdtd_source component=Ez  &&
  center=(1.0 8.7 1.0) size = (2.0 0.0 2.0)
$$ FDTD settings
fdtd_model export_var=density wavel_range=[0.3,1.0] PML_thickness=0.2 &&
    boundary_type=[1,0,1] buffer_x=[0.0 0.0] buffer_y=[0.25 0.5] &&
    buffer_z=[0.0 0.0]  nb_wavel=20 cell_size=[0.02 0.02 0.02] &&
    adjust_xdim = 2.0 parallel=no npe_para=4 &&
    iauto_dt_step=5000 iauto_dt2_step=500 auto_finish=yes  &&
    auto_until_ratio=0.1 &&
    watch_point1=[1.0, 5.75, 1.0] &&
    watch_point2=[1.0, 0.5, 1.0] interface=CLFDTD use_gpu=yes
$$$ Material dispersion coefficients
$
fdtd_dispersion mater=1 order=9 &&
freq_convention=frequency input_unit=MEEP &&
epsinf=2.04035796451 &&
omega1=2.7062678135 gamma1=0.0790945452272 delta_eps1=0.621089076055 &&
omega2=2.78981632422 gamma2=0.0699629831018 delta_eps2=0.738714027602 &&
omega3=2.88518971179 gamma3=0.0871514757114 delta_eps3=0.758047251619 &&
omega4=3.00700118394 gamma4=0.121783389832 delta_eps4=0.908307942556 &&
omega5=3.14059748256 gamma5=0.128444615161 delta_eps5=0.91840909799 &&
omega6=3.27735431341 gamma6=0.130032114231 delta_eps6=1.03948015509 &&
omega7=3.43834397056 gamma7=0.175384768328 delta_eps7=1.81197400746 &&
omega8=3.64220941471 gamma8=0.257470755411 delta_eps8=1.33831807319 &&
omega9=4.10325939911 gamma9=0.349042016522 delta_eps9=0.758536138211
$
fdtd_dispersion mater=6 import=yes &&
freq_convention=omega input_unit=MEEP &&
   file=color_glass_p1.dat
$
fdtd_dispersion mater=4 order=5 &&
  freq_convention=omega &&
  input_unit=SI &&
  epsinf=1.0 &&
  omega1=1.0000e+07 gamma1=7.1405e+13 delta_eps1=2.7088e+18 &&
  omega2=2.4612e+14 gamma2=5.0591e+14 delta_eps2=1.9410e+03 &&
  omega3=2.3457e+15 gamma3=4.7401e+14 delta_eps3=4.7065e+00 &&
  omega4=2.7468e+15 gamma4=2.0525e+15 delta_eps4=1.1396e+01 &&
  omega5=5.2764e+15 gamma5=5.1381e+15 delta_eps5=5.5813e-01

$$$$$$$$$$
start_loop symbol=%ii value_from=1 value_to=2
$real_func symbol=%lit value_from=1.e-10 value_to=1.0e-2
$real_func symbol=%lit value_from=2.5e-3 value_to=6.e-3
real_func symbol=%lit value_from=8.e-3 value_to=1.25e-2
$real_func symbol=%lit value_from=3.e-2 value_to=6.e-2
$real_func symbol=%lit value_from=3.5e-2 value_to=5.e-2
$ Solve for equilibrium condition
newton_par damping_step=5. var_tol=1.e-9 res_tol=1.e-9 &&
  max_iter=100 opt_iter=15 stop_iter=50 print_flag=3 &&
  mf_cpu=4 mf_solver=3
```

```
$scanline=1
parallel_linear_solver
equilibrium
$
$  Gate_TX-1; Gate_Reset-2; Drain_Reset-3
$
newton_par damping_step=3. res_tol=1.e-1 var_tol=1.e-1 &&
  max_iter=30 opt_iter=15 stop_iter=15 print_flag=3 &&
  change_variable=yes mf_cpu=4 mf_solver=3
$ scanline=2
scan var=voltage_3 value_to=5.0 &&
var2=time value2_to=1.e-6
$scan var=voltage_3 value_to=3.0 &&
$var2=time value2_to=1.e-6
$scanline=3
scan var=light value_to=%lit &&
var2=time value2_to=2.e-6
$scanline=4
$ use 10 us to collect signal charge
scan var=time value_to=13.e-6
$
$scanline=5
$ reset briefly to clear up charge at FD
scan var=voltage_2 value_to=5.0 &&
var2=time value2_to=14.e-6
$scan var=voltage_2 value_to=3.0 &&
$var2=time value2_to=14.e-6
$
$scanline=6
$ takes 5 us to clean up
scan var=time value_to=19.e-6
$scanline=7
$ turn reset MOSFET back to off
scan var=voltage_2 value_to=  0.0 &&
var2=time value2_to=21.e-6
$scanline=8
$ wait a little until other transistors are ready
scan var=time value_to=25.e-6
$scanline=9
$ transfer the charge by increasing voltage
scan var=voltage_1 value_to=3.0 &&
var2=time value2_to=26.e-6
$scanline=10
$ allow 5 us for the transfer to complete
scan var=time value_to=31.e-6
$scan11
$ set TX gate voltage back to zero
scan var=voltage_1 value_to=0. &&
var2=time value2_to=32.e-6
$scan12
$ allow reading time
scan var=time value_to=35.e-6
end_loop
end
```

Appendix 3: QE modeling of a BSI pixel by CLFDTD with OptoWizard

```
begin
use_macrofile macro1=my.mac
3d_solution_method 3d_flow=yes
z_structure uniform_zseg_from=0. uniform_zseg_to=0.4 zplanes=5 zseg_num=1
```

```
z_structure uniform_zseg_from=0.4 uniform_zseg_to=0.7 zplanes=4 zseg_num=2
z_structure uniform_zseg_from=0.7 uniform_zseg_to=2.0 zplanes=5 zseg_num=3
load_mesh mesh_inf=CIS3D01.msh zseg_num=1
load_mesh mesh_inf=CIS3D02.msh zseg_num=2
load_mesh mesh_inf=CIS3D03.msh zseg_num=3
output sol_outf=CIS3D.out
$
begin_zmater  zseg_num=1
include  file=CIS3D01.mater
include  file=CIS3D01.doping
light_power light_dir=bottom wavelength=0.4 incident_power=5.0e4
end_zmater
begin_zmater  zseg_num=2
include  file=CIS3D02.mater
include  file=CIS3D02.doping
light_power light_dir=bottom wavelength=0.4 incident_power=5.0e4
end_zmater
begin_zmater  zseg_num=3
include  file=CIS3D03.mater
include  file=CIS3D03.doping
light_power light_dir=bottom wavelength=0.4 incident_power=5.0e4
end_zmater
$
bias_output_near_point variable=potential near_xyz=(0.3 5.0 0.2)
bias_output_near_point variable=potential near_xyz=(1.0 5.2 0.2)
bias_output_near_point variable=potential near_xyz=(1.55 5.2 0.2)
bias_output_near_point variable=potential near_xyz=(2.0 5.2 0.2)
bias_output_near_point variable=potential near_xyz=(2.7 5.2 0.2)
bias_output_near_point variable=potential near_xyz=(3.25 5.2 0.2)
$
more_output space_charge=yes
$
$ FDTD source(s)
$------------------
fdtd_source component=Ez  &&
  center=(1.7 -0.14 1.0) size = (3.4 0.0 2.0)
$ FDTD settings
$-------------------
$ setting at a particular wavelength;
$ using series project for multiple wavelength
$
fdtd_model export_var=density wavel_range=[0.4,0.4] PML_thickness=1.0 &&
    boundary_type=[1,0,1] buffer_x=[0.0 0.0] buffer_y=[1.3 1.2] &&
    buffer_z=[0.0 0.0]  nb_wavel=1 cell_size=[0.02 0.02 0.02] &&
    auto_finish=no fixed_time=10000 &&
    num_zero_optgen_mater=5 &&
    4_zero_optgen_mater=[1 3 4 5 6] &&
    interface=CLFDTD use_gpu=yes parallel=no npe_para=6
$
fdtd_dispersion mater=1 &&
  autofit_singlepole=yes
$
fdtd_dispersion mater=2 &&
  autofit_singlepole=yes
$
fdtd_dispersion mater=3 &&
  autofit_singlepole=yes
$
fdtd_dispersion mater=4 &&
  autofit_singlepole=yes
$
fdtd_dispersion mater=5 &&
  autofit_singlepole=yes
$
$ Material dispersion for Alminium
```

```
$-----------------------------------
fdtd_dispersion mater=6 order=5 &&
  freq_convention=omega &&
  input_unit=SI &&
  epsinf=1.0 &&
  omega1=1.0000e+07 gamma1=7.1405e+13 delta_eps1=2.7088e+18 &&
  omega2=2.4612e+14 gamma2=5.0591e+14 delta_eps2=1.9410e+03 &&
  omega3=2.3457e+15 gamma3=4.7401e+14 delta_eps3=4.7065e+00 &&
  omega4=2.7468e+15 gamma4=2.0525e+15 delta_eps4=1.1396e+01 &&
  omega5=5.2764e+15 gamma5=5.1381e+15 delta_eps5=5.5813e-01
$
fdtd_output_structure &&
  variable=material_num &&
  resolution=(1.0 1.0 1.0) &&
  data_file=materID
$
fdtd_replace_FDTDgrid file=fdtd_grid_for_import.dat
$
$ Settings for QE
$==================
fdtd_define_region &&
    shape=box &&
    point_ll=(0.0 0.0 0.0) &&
    point_ur=(3.4 5.42 2.0) &&
    tag=box_QE
$
$ flux monitor for incident power
fdtd_fieldmonitor &&
   target_region_tag=box_QE &&
   simulation_space=emptyspace &&
   monitor_comp=Efields &&
   FFT=yes &&
   step_start=5000 &&
   resolution=(0.5 0.5 0.5) &&
   tag=QE_monitor_emptyspace
$
$ flux monitor for reflected power
fdtd_fieldmonitor &&
   target_region_tag=box_QE &&
   simulation_space=devicespace &&
   monitor_comp=Efields &&
   FFT=yes &&
   step_start=5000 &&
   resolution=(0.5 0.5 0.5) &&
   tag=QE_monitor_devicespace
$
$ post-processing QE data
$--------------------------
fdtd_data_analysis &&
   operation=QE &&
   operandA_tag = QE_monitor_devicespace &&
   operandB_tag = QE_monitor_emptyspace &&
   scale=1.4705882353e11 &&
   data_file=QE.txt
$ Solve for equilibrium condition
newton_par damping_step=5. var_tol=1.e-9 res_tol=1.e-9 &&
  max_iter=100 opt_iter=15 stop_iter=50 print_flag=3 &&
  mf_cpu=4 mf_solver=3
$scanline=1
equilibrium
end
```